Available online at www.sciencedirect.com
ScienceDirect
Biochimica et Biophysica Acta 1767 (2007) 422–433
Biochimica et Biophysica Acta
BBA
www.elsevier.com/locate/bbabio

Review

Electron and nuclear dynamics in many-electron atoms, molecules and chlorophyll–protein complexes: A review

Vladimir A. Shuvalov *

Institute of Basic Biological Problems, Russian Academy of Sciences, Pushchino Moscow Region, 142290, Russia

Received 14 November 2006; received in revised form 30 January 2007; accepted 1 February 2007
Available online 9 February 2007

Abstract

It has been shown [V.A. Shuvalov, Quantum dynamics of electrons in many-electron atoms of biologically important compounds, Biochemistry (Mosc.) 68 (2003) 1333-1354; V.A. Shuvalov, Quantum dynamics of electrons in atoms of biologically important molecules, Uspekhi biologicheskoi khimii, (Pushchino) 44 (2004) 79-108] that the orbit angular momentum L of each electron in many-electron atoms is $L=mVr=n\hbar$ and similar to L for one-electron atom suggested by N. Bohr. It has been found that for an atom with N electrons the total electron energy equation $E=-(Z^{\text{eff}})^2e^4m/(2n^2\hbar^2N)$ is more appropriate for energy calculation than standard quantum mechanical expressions. It means that the value of L of each electron is independent of the presence of other electrons in an atom and correlates well to the properties of virtual photons emitted by the nucleus and creating a trap for electrons. The energies for elements of the 1st up to the 5th rows and their ions (total amount 240) of Mendeleev' Periodical table were calculated consistent with the experimental data (deviations in average were 5×10^{-3}). The obtained equations can be used for electron dynamics calculations in molecules. For H_2 and H_2^+ the interference of electron–photon orbits between the atoms determines the distances between the nuclei which are in agreement with the experimental values. The formation of resonance electron–photon orbit in molecules with the conjugated bonds, including chlorophyll-like molecules, appears to form a resonance trap for an electron with E values close to experimental data. Two mechanisms were suggested for non-barrier primary charge separation in reaction centers (RCs) of photosynthetic bacteria and green plants by using the idea of electron–photon orbit interference between the two molecules. Both mechanisms are connected to formation of the exciplexes of chlorophyll-like molecules. The first one includes some nuclear motion before exciplex formation, the second one is related to the optical transition to a charge transfer state.

Keywords: Many-electron atoms; Quantum dynamics of electrons in atoms and molecules; Femtosecond spectroscopy; Photosynthetic reaction centers; Non-barrier electron transfer

1. Introduction

The knowledge of the energy and location of electrons in atoms and molecules, of the interaction between electrons and electromagnetic field is of basic interest in physics, chemistry and biology. Quantum physics suggests a number of methods for calculations of the above mentioned properties by using the Schrödinger equation [1–5]. However in spite of very well developed and sophisticated approaches the correlation between the calculation and experimental data is not better than 1–1.5% for the outer electrons that are important for chemical and biological bonds.

The development of quantum electrodynamics by Feynman [6,7] and other groups (see [8]) has allowed to formulate the main principles for the interaction between electrons and nuclei via virtual photons. However, the problem of many-electron atoms has not been yet completely solved by this theory until now.

The aim of the first part of this paper is to consider the Coulomb interaction between an electron with a charge e_o and

Abbreviations: ΔA, light-minus-dark absorbance changes; BChl, bacteriochlorophyll; B_A and B_B, monomeric BChls located at the A- and B-branch, respectively; ET, electron transfer; FT, Fourier transform; fs, femtosecond; P, primary electron donor; ps, picosecond; RC, reaction center; ($Z^{\text{eff}}=ZNk-\Sigma_i\Sigma_j\, r/r_{ij}$), is an effective Coulomb interaction of nucleus and electrons in an atom

* Corresponding author. Tel.: +7 4967 733601; fax: +7 4967 330532.
E-mail address: shuvalov@issp.serpukhov.su.

0005-2728/$ - see front matter © 2007 Elsevier B.V. All rights reserved.
doi:10.1016/j.bbabio.2007.02.002

the nucleus with a charge Ze_o in many-electron atoms by using some modification of quantum electrodynamics approach with further application to the molecules. In the second part the methodology is used to describe the charge transfer processes in photosynthetic reaction center complexes.

The energy of Coulomb interaction (E_c) between an electron and the nucleus in atom is expressed by following equation:

$$E_c = -Ze_o^2/r, \quad (1)$$

where r is the distance between the charges. This equation is valid for atomic distances and is effectively used for the energy calculations of atoms and molecules [1–5]. However, although the expression is formally correct, it does not reveal the details of the interactions which important for an understanding of the quantum behavior of elementary particles involved in the interaction between electrons and the nucleus. The details become evident when we consider the interaction between the charges within the framework of an electromagnetic field of the photons as the carriers of this field.

For two interacting electrons the virtual photon exchange is very well known [6–8] and expressed by the exchange of momentum of the three interacting particles. Charge–photon interaction between an electron and nucleus is not so simple. It has been shown [9,10] that the angular momentum (L_i) for each electron in a many-electron atom is similar to that one found by N. Bohr for one-electron atom, i.e.:

$$L_i = mV_i r_i = n, \quad (2)$$

where m, V_i and r_i are mass, velocity and distance to the nucleus, respectively, of an electron i; n=1,2,3...is a main quantum number; $\hbar$ is the Planck constant. Application of this equation gives a result with remarkable agreement with experimental data [9,10]. The Eq. (2) means that any electron in a many-electron atom has an L_i that is independent of the presence of other electrons and that this L_i is determined by the fundamental properties of an electron–photon interaction which we discuss below. The Eq. (2) is very much different from the standard quantum mechanic equation considering $L^2=l(l+1)\hbar^2$, where l is an quantum number of the angular momentum equal to 0, 1...($n-1$). This difference leads to different calculations of the energy of an electron within the atom. As it is discussed below the Eq. (2) corresponds to the exchange of virtual photon spin ($\hbar$) with an electron angular momentum which becomes equal to $\hbar$ or $n\hbar$.

The simplest way to explain the main part of the Coulomb interaction between the nucleus and an electron expressed by Eq. (1) is to consider the electromagnetic field emitted by the nucleus and interacting with an electron. Remarkably, the small distance between the nucleus and electrons in an atom is comparable with an electromagnetic field wavelength, and therefore leads to the suggestion that the nucleus emits spherical and/or cylindrical photons interacting with electrons. The result of the approach is discussed and applied to many-electron atoms with remarkable agreement with an experiment.

In the second part of this paper the virtual photon theory is applied to molecules, including aromatic compounds with long conjugated π-electron systems, and to chlorophyll–protein complexes.

2. Theory

2.1. Many-electron atoms

The difference between a quantum mechanical expression for L^2 and the Eq. (2) appears to be due to the consideration of two things in the former approach: electron wave properties and Coulomb interaction between an electron and the nucleus in an atom. On the other hand, taking into account that the Coulomb field is determined by virtual photons emitted by the nucleus and having a spin (equal to $\hbar$), the second new approach is based on the following: a permanent exchange of the photon spin with the electron angular momentum leads to the equalization of both in agreement with the Eq. (2).

Formally the electron-field interaction can be written using the Eq. (2) in the following way. For the first Bohr orbit we have for an electron velocity (V), distance (r), main quantum number (n) and photon wavelength (λ): $V=V_o=c/137$; $r=r_o=$ 0,529117249 Å; $n=1$; $\lambda=\lambda_o=2\pi r_o$. Using Eq. (2) one can find that the kinetic energy (E_k) of an electron is as follows:

$$E_k = mV_o^2/2 = V_o/2r_o = hc/(2\lambda_o 137) = hv_o/(2\cdot 137) \quad (3)$$

According to the virial theorem and the Bohr expressions for one electron atom the potential energy (E_p) of an electron is always equal to $-2E_k$. Thus one can see from Eq. (3) that $-E_p$ is equal to the energy of quantum with $\lambda_o=2\pi r_o$ multiplied by the fine structure constant (1/137):

$$E_p = -hc/(\lambda_o 137) \quad (4)$$

Thus, the idea of an electron-field interaction is formally expressed via a virtual cylindrical and/or spherical photon with $\lambda_o=2\pi r_o$ and the energy of 3727 eV (equal to the electron mass in eV multiplied by 1/137) emitted by a nucleus. The photon creates a trap for an electron in an atom with formation of negative potential energy of −27.21 eV (=−3727eV/137) at the distance r_o from the nucleus. It should be noted that here and below all calculated energies are consistent with the Coulomb interaction energy (1).

Since the general important rule that $E_p=-2E_k$, is satisfied, the total energy (E) for electrons with the same n is equal to $E_p/2$. For many (N) electrons with the same n in an atom the equations for calculation of minimal electron potential energy and the corresponding total energy E, as well as the distance (r from the nucleus) are based on Eq. (2) as outlined in [9,10]. For kinetic, potential and total energies we have:

$$E_k = Nn^{2\,2}/(2mr^2), \quad (5)$$

$$E_p = -Z^{\text{eff}}e^2/r, \quad (6)$$

$$E = E_k + E_p, \quad (7)$$

where Z^{eff} is a coefficient of effective Coulomb interaction of charged particles in the atom:

$$Z^{\text{eff}} = ZNk - \Sigma_i \Sigma_j r/r_{ij}, \quad (8)$$

where r is a distance of any of the N electrons with the same $n=n_e$ from the nucleus; r_{ij} is the distances between each electron i and the other; Z is a remaining charge of the nucleus that is shielded by lower lying electrons with $n<n_e$; k is a coefficient correcting the incomplete shielding of nuclear charge by low lying electrons with $n<n_e$ (for helium $k=1$). The Eq. (8) is based on the general suggestion that in a many-electron atom the electrostatic field is created not only by the nucleus but electrons as well, which interact with the nucleus via virtual photons. The total Coulomb interaction determined by Eq. (8) is an integral feature of an atom where the electrons are trapped with a total energy according to Eq. (7).

To use Eq. (8) it is necessary to find the value of the expression $\Sigma_i\Sigma_j\ r/r_{ij}$. A reasonable result is obtained by the suggestion [9,10] that two electrons with $n=1$ move synchronously on two orthogonal orbits to get minimal potential energy. For this case two predominant locations for electrons with angle of 90 ° and of 180 ° with the nucleus in the center are in good correlation with experiment (see Appendix). For $n=2$ eight electrons move synchronously on four orthogonal orbits and are predominantly located in the corners of a cub with the nucleus in the center. For $n=3$ eighteen electrons move synchronously on six orthogonal orbits and are predominantly located in the complicated figure with the same distance from the nucleus in the center [9,10]. Taking into account these figures one can find an average reciprocal distance between electrons expressed in the form of r/r_{ij} which is necessary for further calculation: 0.6035535 for $n=1$ (90 ° and 180 ° each to other with nucleus in center); 0.705033 for $n=2$ (corners of cub); 0.8398 for $n=3$ and so on. Furthermore, the average value r/r_{ij} is multiplied by the amount of interactions between the electrons to get $\sum_i\sum_j\ r/r_{ij}$ required for the calculation of many-electron atom energy [9,10] (see Appendix for other details).

Furthermore, creating differential equation from (5–8) and taking into account that $\Sigma_i\ \Sigma_j\ r/r_{ij}$ does not depend on r, one can find minimal energies and corresponding distances allowed in an atom [9,10]:

$$E = -(Z^{\text{eff}})^2 e^4 m/(2n^{22}N) = -13,6056981(Z^{eff})^2/(n^2N)\,(eV), \quad (9)$$

$$r = n^{22}N/(Z^{eff}e^2m) = r_o n^2 N/Z^{\text{eff}} = 0,529117249\,n^2N/Z^{\text{eff}}\,(\mathring{A}), \quad (10)$$

The Eqs. (5)–(10) prove again the general rule for allowed states in many electrons atoms: $E_p=-2E_k$.

Thus, for many (N) electrons with the same n in an atom the total minimal potential energy E_p (Eq. (4)) can be modified according to (9) as follows:

$$E_p = -(Z^{\text{eff}})^2 h\nu_o/(137n^2N) \quad (11)$$

One can see that the potential energy (E_p) is proportional to $h\nu_o/137$, the energy of virtual photon with $\lambda_o=2\pi r_o$ multiplied by the fine structure constant. In other words, the electron potential energy appears to be determined by the virtual photon energy emitted by nucleus. An increase of the nucleus charge Z leads to an increase of the virtual photon energy ($h\nu$ is proportional to Z) and of the electron trap energy (proportional to Z as well). The total increase of negative electron potential energy is proportional to Z^2. An increase of n leads to an increase of the number of photon waves (proportional to $2n^2$ but see below) and an increase of λ for each wave (proportional to n^2) with constant total photon energy emitted by the nucleus. For $n=1$ and $Z=1$ two photon waves, corresponding to the emission of two virtual photons with total energy of 2·3727 eV = 7454 eV, accept two electrons. For $n=2$ eight waves are able to accept eight electrons. For $n=3$ eighteen waves accept eighteen electrons, and so on. In the presence of other electrons with the same n the potential energy is dependent not only on the nuclear electric field but on the electron field as well ($Z\approx Z^{\text{eff}}$). It is not clear if this effect is due to either the electric field of electrons directly or to a change of the electric field of the nucleus in the presence of interacting electrons.

A similar situation can be proposed for the orbit angular momentum of an electron. Since the photon spin is $\hbar$, one can suggest that this spin is exchanged with the orbit angular momentum (getting the same $\hbar$) of an electron ($n=1$) trapped by the photon electromagnetic field. For an electron with $n>1$ the angular momentum is $n\hbar$. It means that for electrons with $n=2$ two photon spins are exchanged with the electron angular momentum, for $n=3$ three photon spins are exchanged with the electron angular momentum, and so forth. This feature is not simple since for $n=2$ we have claimed that 8 photon waves (energy of emitted photons is $8\cdot3727/n^2=7454$ eV) accept 8 electrons but at the same time two photon spins are exchanged with the electron angular momentum. It means that for $n=2$ two photon waves are interacting with the creation of one electron–photon orbit accepting two electrons with $L=2\ \hbar$. As a result there are 4 electron–photon orbits accepting 8 electrons with $n=2$. An analogous situation occurs for $n=3$ when 18 photon waves (energy of emitted photons is $18\cdot3727/n^2=7454$ eV) accept 18 electrons but three photon waves are interacting with the creation of one electron–photon orbit accepting three electrons with $L=3\ \hbar$. As a result there are six electron–photon orbits accepting 18 electrons with $n=3$, and so on. Please note that in all cases the total photon energy emitted by the nucleus is constant and equal to 7454 eV (see Appendix for other details).

3. Calculations

3.1. Many-electron atoms

Using Eq. (9) one can find that the calculated total energy for 8 electrons with $n=2$ of Ne is equal to –952.705 eV, the sum of the experimental ionization potentials for these 8 electrons is 953.61 eV [11]. The calculated energy for 7 electrons with $n=2$ of F is –659.65 eV, the sum of experimental data is 658.65 eV, etc. (see Tables 1 and 2). The energies and electron–nucleus

Table 1
Calculated energies and distances for N electrons in atoms of Mendeleev' Periodical table for rows I–V and their ions (Eqs. (9) and (10)) in comparison with total ionization potential of these electrons [11] and atomic radius [32]

Element or its ion	Calculated energy for N electrons in atom, eV	Ionization potential for N electrons in atom, eV [11]	Deviation of calculation from an experiment	Distance of an electron from nucleus, Å (Atomic radius, Å [32])
$^{1}He^{2+}{}_{2e}$	−78,4745	79,005	$6{,}7\times10^{-3}$	0,3115 (0,31)
$^{1}Be^{4+}{}_{2e}$	−372,14	371,61	$1{,}4\times10^{-3}$	0,1430
$^{2}Ne^{8+}{}_{8e}$	−952,705 (k=1,04805)	953,61	9×10^{-4}	0,3576 (0,38)
$^{3}Kr^{26+}{}_{18e}$	−12091,25 (k=1,08532)	12106	0,0012	0,2259
$^{3}Zn^{20+}{}_{18e}$	−6121,9 k=(1,104754)	6163,22	0,0067	0,3175
$^{3}Cu^{19+}{}_{16e}$	−5274,92 (k=1,10874)	5311,07	0,0068	0,3225
$^{3}Ni^{18+}{}_{16e}$	−4568,17 (k=1,1134)	4614,89	0,01	0,3465
$^{3}Co^{17+}{}_{15e}$	−3911,801 (k=1,11840)	3948,07	0,0092	0,3626
$^{3}Fe^{16+}{}_{14e}$	−3324,92 (k=1,12454)	3351,75	0,008	0,3799
$^{3}Mn^{15+}{}_{13e}$	−2789,01 (k=1,130108)	2818,83	0,01	0,3997
$^{3}Ar^{8+}{}_{8e}$	−559,60 (k=1,2177)	577,75	0,031	0,7000 (0,71)
$^{3}Cl^{7+}{}_{7e}$	−403,1 (k=1,24162)	408,883	0,014	0,7716 (0,79)
$^{3}S^{6+}{}_{6e}$	−277,62 (k=1,27198)	276,355	0,0046	0,8607 (0,88)
$^{3}P^{5+}{}_{5e}$	−176,25 (k=1,30167)	176,929	0,0039	0,9862 (0,98)
$^{3}Si^{4+}{}_{4e}$	−103,74 (k=1,350394)	103,1324	0,0059	1,1497 (1,11)

The indexes (for example $^{2}Ne^{8+}{}_{8e}$) mean: ^{2}Ne indicates the electrons for neon with n=2; Ne^{8+} indicates a charge of nucleus after shielding by lower lying electrons; Ne_{8e} indicates the amount (N) of electrons. The coefficient k corrects the incomplete shielding of nuclear charge by lower lying electrons (for helium k=1). This coefficient can be find for ions with only one electron with corresponding n using (9) or calculated according to [10].

distances for elements of the 1st up to the 5th rows and their ions (total amount 240) of Mendeleev' Periodical table were calculated consistent with the experimental data [9,10]. The deviations in average were 5×10^{-3} [9,10]. In other words, the uncertainty in the calculations of the energies was proportional to the energies of valence electrons. For small energies in some cases the deviation was about 5×10^{-5} (Li^{+} [9]) or the difference between the calculations and the experimental data was about 0.01 eV in this case.

3.2. Molecules

It is possible to show that the principle of electron–nucleus interaction via virtual photon can be applied to understand the molecule construction. It was suggested [9,10] that in simple molecules like H_2 and H_2^+ the interaction between two atoms is due to the interference of four cylindrical electron–photon orbits (with two orthogonal electron–photon orbits in each atom) including the virtual photons emitted by two nucleus with $\lambda_o=2\pi r_o$ (Fig. 1). Since these photons provide the traps for electrons at the distance of r_o (0.529 Å) from nucleus the interference of two electron–photon orbits of two atoms at their edges creates a new trap for an electron with an increased negative potential energy. These traps provide an additional negative potential energy in the molecule with respect to the isolated atoms. The position of new traps determines the distance between nuclei: $2r_o$ for H_2^+ (1.058 Å) and $2r_o/1.414$ for H_2 (0.748 Å) (see Fig. 1). These estimations are in good agreement with experimental data (1.06 Å and 0.741 Å, respectively). For energy calculations the deepness of the new traps should be estimated. According to the energy of Coulomb interaction for an electron located just in the middle between two nuclei in H_2^+ the trap deepness of $-2\cdot27.21$ eV should be observed (Fig. 1, upper panel). Similar trap deepness should be observed for H_2 at two interference points of two pairs of waves (Fig. 1, lower). Taking into account that electrons can move around photon waves the total potential and kinetic energies can be calculated for H_2^+ and H_2 in reasonable agreement with experiment values.

For atoms having electrons with $n>1$ the situation is more complicated and the arrangement of such electrons in an atom should be taken into account [9,10]. For example, the Li_2 molecule appears to have the same interaction of four electron–photon orbits but they are not completely orthogonal according to the cub arrangement of electrons with n=2. Taking this into account one can find a reasonable agreement with an experiment.

3.3. The molecules with conjugated π-electron systems including photosynthetic pigments

For molecules with conjugated π-electron systems the general suggestion that an electron interacts with nuclei via virtual resonance photon can be applied. For such molecule a new electron–photon orbit (resonance) can be proposed with λ equal to the length of the conjugated system. The Eq. (4) for the electron potential energy of the hydrogen atom ($E_p=-hc/(\lambda_o 137)$) shows a principle method for the calculation using the wavelength of the emitted photon. According to this equation the potential energy is determined by the photon energy multiplied by the fine structure constant. If in the conjugated system the virtual photon emitted by effective Coulomb interaction of charged atoms of the system determines the potential energy of the electron trap, in the Eq. (4) the λ_o should be replaced by λ of the conjugated system:

$$E_p = -hc/(\lambda 137). \quad (12)$$

Since the potential energy (12) is only determined by λ and independent of n, and the general rule that $E_p^{res}=-2\ E_k^{res}$,

Table 2
Calculated energies and distances for N electrons in atoms of Mendeleev' Periodical table for row II and their ions (Eqs. (9) and (10)) in comparison with total ionization potential of these electrons [11] and atomic radius [32]

Element or its ion	Calculated energy for N electrons, eV	Ionization potential for N electrons, eV [11]	Deviation of calculation from an experiment	Distance of electrons from nucleus, Å	Atomic radius, Å [32]
$^{2}Ne^{8+}{}_{8e}$	−952.705 (N=8) (k=1.04805)	953.61	9×10^{-4}	0.3576	0.38
$^{2}Ne^{8+}{}_{7e}$	−935.78 (N=7)	932.05	4×10^{-3}	0.3375	
$^{2}Ne^{8+}{}_{6e}$	−894.84 (N=6)	891.087	4.2×10^{-3}	0.3196	
$^{2}Ne^{8+}{}_{5e}$	−827.207 (N=5)	827.637	5×10^{-4}	0.3034	
$^{2}Ne^{8+}{}_{4e}$	−730.35 (N=4)	730.517	2.3×10^{-4}	0.2888	
$Ne^{8+}{}_{3e}$	−601.74 (N=3)	604.74	4×10^{-3}	0.2755	
$^{2}Ne^{8+}{}_{2e}$	−438.84 (N=2)	446.375	0.017	0.2618	
	−444.40 (N=2) (He configuration)		4.4×10^{-3}		
$^{2}Ne^{8+}{}_{1e}$	(N=1)	239.0989		0.2524	
$^{2}F^{7+}{}_{7e}$	−659.65 (N=7) (k=1.05411)	658.65	1.2×10^{-3}	0.4020	0.42
$^{2}F^{7+}{}_{6e}$	−643.68 (N=6)	642.68	2.2×10^{-3}	0.3768	
$^{2}F^{7+}{}_{5e}$	−605.85 (N=5)	607.26	2.3×10^{-3}	0.3668	
$^{2}F^{7+}{}_{4e}$	−543.63 (N=4)	543.73	1.8×10^{-4}	0.3347	
$^{2}F^{7+}{}_{3e}$	−454.46 (N=3)	456.46	4.7×10^{-3}	0.3171	
$^{2}F^{7+}{}_{2e}$	−335.83 (N=2)	342.83	0.019	0.2990	
	−340.69 (N=2) (He configuration)		4.8×10^{-3}		
$^{2}F^{7+}{}_{1e}$	(N=1)	185.196		0.2868	
$^{2}O^{6+}{}_{6e}$	−433.68 (N=6) (k=1.06208)	433.10	1.3×10^{-3}	0.4590	0.48
$^{2}O^{6+}{}_{5e}$	−418.79 (N=5)	420.06	3×10^{-3}	0.4264	
$^{2}O^{6+}{}_{4e}$	−384.32 (N=4)	384.94	1.6×10^{-3}	0.3981	
$^{2}O^{6+}{}_{3e}$	−327.74 (N=3)	330.00	6.8×10^{-3}	0.3734	
$^{2}O^{6+}{}_{2e}$	−250.69 (N=2) (He configuration)	252.02	5.2×10^{-3}	0.3486	
$^{2}O^{6+}{}_{1e}$		138.1197		0.3321	
$^{2}N^{5+}{}_{5e}$	−265.95 (N=5) (k=1.07295)	266.95	3.6×10^{-3}	0.5351	0.56
$^{2}N^{5+}{}_{4e}$	−252.40 (N=4)	252.42	6×10^{-5}	0.4913	
$^{2}N^{5+}{}_{3e}$	−221.55 (N=3)	222.82	5.7×10^{-3}	0.4541	
$^{2}N^{5+}{}_{2e}$	−174.37 (N=2) (He configuration)	175.90	5.6×10^{-3}	0.4179	
$^{2}N^{5+}{}_{1e}$	(N=1)	97.8902		0.3945	
$^{2}C^{4+}{}_{4e}$	−147.89 (N=4) (k=1.08863)	148.03	9×10^{-4}	0.6418	0.67
$^{2}C^{4+}{}_{3e}$	−135.90 (N=3)	136.77	6.4×10^{-3}	0.5798	
$^{2}C^{4+}{}_{2e}$	−111.73 (N=2) (He configuration)	112.38	5.8×10^{-3}	0.5221	
$^{2}C^{4+}{}_{1e}$	(N=1)	64.4939		0.4860	
$^{2}B^{3+}{}_{3e}$	−70.82 (N=3) (k=1.1132)	71.38	7.9×10^{-3}	0.8032	0.87
$^{2}B^{3+}{}_{2e}$	−62.77 (N=2) (He configuration)	63.085	4.9×10^{-3}	0.6966	
$^{2}B^{3+}{}_{1e}$	(N=1)	37.93064		0.6338	
$^{2}Be^{2+}{}_{2e}$	−27.543 (N=2) (He configuration) (k=1.1570)	27.534	3.2×10^{-4}	1.0516	1.12
$^{2}Be^{2+}{}_{1e}$	(N=1)	18.21116		0.9485	
$^{2}Li^{1+}{}_{1e}$	(N=1)	5.39172		1.6810	1.67

The indexes (for example $^{2}Ne^{8+}{}_{8e}$) mean: ^{2}Ne indicates the electrons for neon with n=2; Ne^{8+} indicates a charge of nucleus after shielding by lower lying electrons; Ne_{8e} indicates the amount (N) of electrons. The coefficient k corrects the incomplete shielding of nuclear charge by lower lying electrons (for helium k=1). This coefficient can be find for ions with only one electron with corresponding n using Eq. (9) or calculated according to [10].

$E^{res}=E_p^{res}+E_k^{res}$ is probably valid for this case as well, there is only one allowed state with those energies. Furthermore, only the transition from the state with the total energy E^{res} to a released electron state ($E^{res}=0$, but the atom energies are not equal to 0) can be observed. For example, the benzene molecule has a conjugated system with a radius (r) of ~1.5 Å and a length of ~9.42 Å ($2\pi r$). From that one can find that the created electron resonance trap has $E^{res}=-4.8$ eV. If the energy of 4.8 eV is applied to the molecule by an incident photon (with λ=259 nm) one can increase E_k up to $E_k=-E_p$ and release an electron from the resonance trap (but not from other traps in the molecule). Experimental absorption band for benzene is around 260 nm. The coincidence of the calculated and the experimental data for such a case means that optical transition occurs between the energy level of an electron trapped by the conjugated system and the level corresponding to the released electron. Upon excitation the electron kinetic energy is increased up to 9.6 eV (equal to $-E_p^{res}$) and some probability emerges for an electron to move away from an aromatic molecule. In agreement with this expectation the formation of a solvated electron upon il-

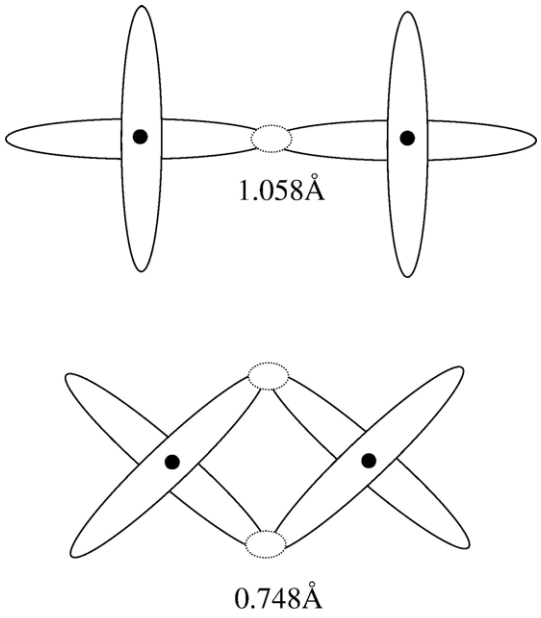

Fig. 1. Schematic representation of the interference of the orthogonal electron–photon orbits with a length of $2\pi r_o$ (r_o = 0.529 Å) in molecules of H_2^+ (upper) and H_2 (lower). Since in H_2 two electrons populate the orbits, two points of the interference of four electron–photon orbits are discerned (by dotted circles) in contrast to H_2^+ where only one point of the interference is observed. Distances between nuclei are in good correlation with an experiment (1.06 and 0.741 Å, respectively).

lumination of aromatic molecules at low temperature is described in literature [12].

An important example of the calculations using a similar approach is related to the photosynthetic pigments. The chlorophyll molecule has two lengths of the conjugated π-electron system: the long one with the length of 24.23 Å and the short one of 19.69 Å. Using Eq. (12) one can find that E^{res} = −1.865 eV and −2.296 eV, respectively. This corresponds to the calculated transitions at 665 nm (Q_y transition) and 540 nm (Q_x transition), respectively, in good correlation with the experimental data. Again the transitions occur from the energy level of an electron trapped by the conjugated system and the level corresponding to the released electron. Upon excitation the kinetic energy of an electron is increased up to about 3.6 eV (Q_y) that can provide electron tunneling through the barriers of the molecule. This property of the conjugated system might be important for electron transfer (ET) reactions from the excited chlorophyll to the neighbor chlorophyll in the photosynthetic reaction center. To calculate the Soret' band transitions we should probably consider the trapping of two electrons by a resonance trap.

Retinal molecule of visual rhodopsin has about 12 conjugated bonds. If two bonds length is 2.3 Å the length of conjugated system is about 13.8 Å. By using Eq. (12) one can find that E^{res} = −3.252 eV. This corresponds to the transition at 381 nm from the energy level of an electron trapped by conjugated system to the level corresponding to the released electron. The experimental data show the transition at 380 nm for all-trans-retinal.

4. The mechanism of non-barrier electron transfer between molecules

The mechanism of non-barrier electron transfer between molecules is always related to the coupling between electron and nuclear dynamics. The conventional theory of the coupling, mostly for relaxed states, is outlined in a number of papers (for review see [13,31]). Some new aspects including nuclear dynamics in the fs time domain are described below.

According to Fig. 1 the interference of the electron–photon orbits of two atoms in H_2 leads to the creation of new traps for an electron in the molecule with increased negative potential energy. Thus, in the molecule an electron belongs to two atoms and can be transferred from one to another without any addition barrier. A similar idea can be applied to the interaction between molecules especially if these molecules posses long conjugated systems. The interference of the electron–photon orbits of two molecules that are located at short mutual distance can be responsible for non-barrier electron transfer. The formation of excimers and exciplexes in solution of dyes [14,15] is an example of such an interaction. The electron density is shifted from one molecule to another during the excited state of a dimer created after excitation of one monomer. If a dimer with slightly shifted electron density from one molecule to another due to different redox potentials of the monomers, is formed in a chemical or biological structure in the dark, the optical transition occurs to the charge transfer (CT) state. Thus, two mechanisms for non-barrier ET can be observed between molecules with long conjugated systems:

(i) nuclear motions leading to the formation of the dimer after excitation of one monomer and subsequent electron-density shift from one molecule to another;
(ii) formation of the dimer in the dark with some density shift from one monomer to the other one due to slightly different redox potentials of monomers; two monomers in the dimer attract each other due to Coulomb interaction, and the transition to the charge transfer state is observed upon excitation.

The mechanism (i) requires some time for nuclear motions before the dimer formation, while the mechanism (ii) is realized simultaneously with light absorption.

4.1. Electron transfer reactions in photosynthetic reaction centers

The principles described above are realized in the non-barrier ET between chlorophyll-like molecules in photosynthetic reaction centers.

4.1.1. (A) Bacterial reaction centers

The bacterial reaction centers (RCs) after excitation with fs laser pulses exhibit the nuclear motions of the primary electron donor in the fs time domain that lead to formation of an exciplex with a charge transfer from one molecule to another one. The experimental evidences for that mechanism are described below.

The primary electron donor in bacterial RCs is a dimer P of two bacteriochlorophyll (BChl) molecules (P_A and P_B) with distances between the centers of ~7 Å and between the conjugated systems of ~3.5 Å [16,17]. The primary electron acceptor is a monomeric BChl (B_A) separated from P by ~4 Å (edge-to-edge) (Fig. 2). The formation of P* gives rise to stimulated emission at around 920 nm, that decays within ~1.5 ps at 90 K and is accompanied by the formation of the product state $P^+B_A^-$ characterized by a band at 1020 nm belonging to B_A^- [18,19]. The formation of the wave packet on the P* potential energy surface in the fs time domain leads to oscillations of the stimulated emission with a frequency of 130–150 cm^{-1} in P* and a reversible shift of the emission maximum from 895 nm at 0 delay to 940 nm at 120 fs delay and so on [18–21]. At 120 fs delay the electron density is reversibly shifted (~25%) from P* to B_A with the formation of the B_A^- band at 1020 nm [18,19,22]. Such an electron density shift that is correlated with the appearance of the 940-nm emission from P* strongly indicates that the long-wavelength emission is related to exciplex formation in P*. In agreement to that other recent studies showed that the conversion of the excited state P* into the charge separated state starts in a dimer where increased electrical dipole is formed in the excited state of P* [23].

In order to obtain more information on the origin of the 130–150 cm^{-1} mode in nuclear motions, we studied fs oscillations in RCs of the double mutant YM210L/FM197Y of *Rb. sphaeroides*. In a single mutant YM210L(W) [24] the kinetics of the stimulated emission of P* demonstrate the absence of a stabilization of $P^+B_A^-$ within the ps time domain (Fig. 3, thin lines). Seven periods of reversible electron transfer from P* to B_A (with period of ~260 fs) are observed showing some nuclear motion coupled to ET in the absence of the stabilization of $P^+B_A^-$ [24]. The second mutation introduces a new tyrosine residue at the position M197 that was found to donate a hydrogen bond to the acetyl carbonyl group of the ring I of P_B [25].

Fig. 3 (thick lines) shows that in the double YM210L/FM197Y mutant of RCs the frequency of the initial oscillations in the kinetics of stimulated emission from P* at 935 nm and in the product formation kinetics at 1020 nm (not shown) is shifted from 150 cm^{-1} to ~100 cm^{-1}. This frequency shift to a lower value seems to originate from an increase of the effective mass of some part of the oscillating molecular group (retarding its motion) and can be tentatively rationalized in terms of a hydrogen bond formation. An increase of the effective mass of the acetyl group of the pyrrol ring I of P_B due to its involvement in the hydrogen bond with OH-TyrM197 would then imply that

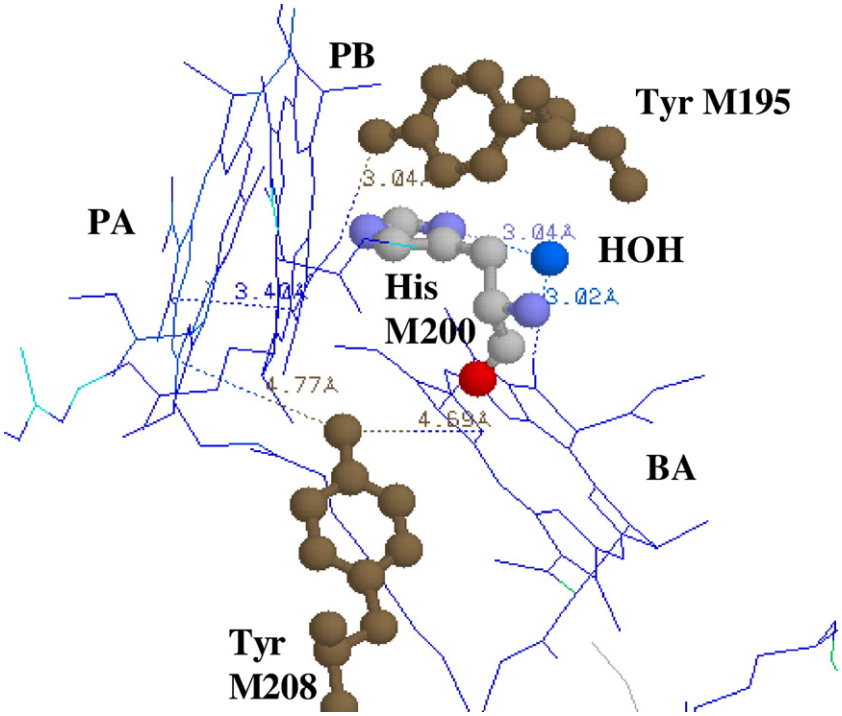

Fig. 2. View (Brookhaven protein databank, number 1PRC) of special pair of bacteriochlorophylls P_A and P_B, monomeric bacteriochlorophyll B_A of *Rps. viridis* RCs. His M200 liganding Mg of P_B is connected by hydrogen bonds via H_2O to oxygen of keto carbonyl group of ring V of B_A. Thus P_B is connected to B_A via a sequence of following polar groups: Mg(P_B)–N–C–N(His M200)–H–O–H(water)–O═B_A which can represent a pathway for the electron transfer from P* to B_A. The rotation of the water molecule in such a system with 32 cm^{-1} frequency is induced by the electron flow from P* to B_A. The OH group of OH-TyrM195 (FM197 in *Rb. sphaeroides*} forms an hydrogen bond with the acetyl group of the pyrrol ring I of P_B. An increase of the effective mass of the acetyl group of the pyrrol ring I of P_B due to its involvement in the hydrogen bond with OH-TyrM197 would mean that the pyrrol ring I of P_B is involved in the nuclear motion induced by fs-excitation of P. This is supported by the lower frequency shift in the double mutant YM210L/FM197Y of *Rb. sphaeroides* (see Fig. 3). Reorientation of the surrounding polar group like $O^{\delta-}H^{\delta+}$ of TyrM210 (M208 in *Rps. viridis* RCs) provides the stabilization of the product $P^+B_A^-$. In the absence of YM210 in mutants YM210W(L) the oscillations with period of 215 fs at 935 nm are not perturbed within ~1.5 ps (Fig. 3). However the stabilization of the product $P^+B_A^-$ is completely blocked in the mutants (see text for further discussion).

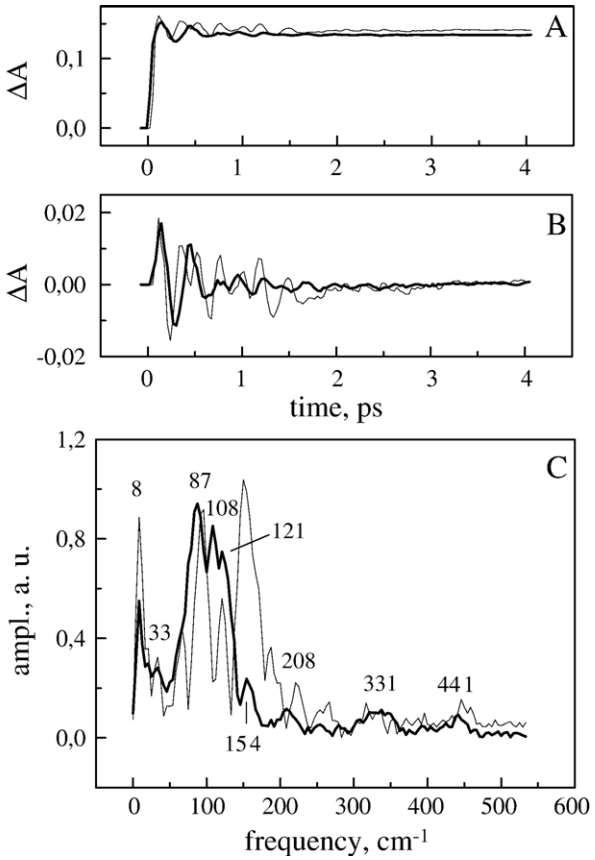

Fig. 3. Femtosecond kinetics of ΔA (A), its oscillatory part (B) and the spectrum of Fourier transform of the oscillatory part (C) for the 935-nm band in RCs of mutant YM210L (thin) and double mutant YM210L/FM197Y (thick) of *Rb. sphaeroides* in glycerol-TT buffer at 90 K. RCs were excited by 20-fs pulses at 870 nm. (From Yakovlev et al., 2007, in press).

the pyrrol ring I of P_B is involved in the nuclear motion induced by excitation of P with fs laser pulses. A similar low frequency shift has been observed for the stimulated emission from P* in RCs of the single FM197H mutant of *Rb. sphaeroides* [21] that is also possibly due to formation of a new hydrogen bond between the acetyl carbonyl of ring I of P_B and HisM197. In the symmetrical HL168F mutant, where the natural hydrogen bond between the acetyl carbonyl group of ring I of P_A and HL168 was removed, the frequency changes were not so evident [26].

Based on this assumption, the oscillations with frequencies in the range of 130–150 cm^{-1} found in the kinetics of both stimulated emission from P* and the product $P^+B_A^-$ reflect the motion of P_B with respect to P_A in the space of overlapping of rings I of P_A and P_B. One of the consequences of this motion might be the formation of an excited molecular complex by charge transfer interaction similar to well known appearance of excimer and exciplex complexes between aromatic cycles of the excited dyes in a solution [15]. These molecular dimers formed in the excited state of the dyes are characterized by a parallel orientation of the conjugated π-electron systems of two monomers with partial charge transfer from one molecule to other one. Excimer and exciplex formation is accompanied by a long-wavelength shift of the fluorescence with respect to the monomeric dye. It is reasonable to expect the formation of such excited dimers between two (B)Chls in P870 (and possibly in P700 of photosystem I of green plants) when ring I of P_B is shifted to a position closest to ring I of P_A. Then the appearance of the long-wavelength stimulated emission from P* at 940 nm at 120 fs delay could be interpreted as a result of a "dynamic" formation of the exciplex between P_A and P_B. This suggestion is strongly supported by the electron density shift from P* to B_A with the formation of the band at 1020 nm at the same delay. According to the idea of the resonance electron–photon orbits in the conjugated π-electron systems the excimer and exciplex formation can be considered as an interference of two orbits of two monomers in the dimer when the distance between them is close enough.

The dynamic stabilization of $P^+B_A^-$ is of interest for further discussion. Two possibilities can be considered: (i) an electron is transferred from P* to B_A into a higher vibrational level on the $P^+B_A^-$ surface with subsequent vibrational relaxation to the lowest level according to well known models for electron transfer (see [13] for refs.); (ii) stabilization due to a reorientation of surrounding groups when $P^+B_A^-$ is reversibly formed. In the later case the symmetrical arrangement of two potential energy surfaces P* and $P^+B_A^-$ can be realized with maximal possible rate of ET from P* to B_A. When the nuclear motion on the P* surface approaches the crossing point between the two surfaces, both states P* and $P^+B_A^-$ are present [18,19], and the wavepacket goes back to the P* surface if there is no additional changes in nuclear position. However non-coherent nuclear changes can be induced by reorientation of the surrounding polar group like $O^{\delta-}H^{\delta+}$ of TyrM210 (Fig. 2). In the absence of YM210 in the mutants YM210W(L) of *Rb. sphaeroides* the oscillations with period of 215 fs at 1020 nm are not perturbed within ~1.5 ps (Fig. 3). In these mutants the stabilization of the product $P^+B_A^-$ is completely blocked in the ps time domain. This finding would mean that the motion of $H^{\delta+}$ of OH-TyrM210 toward B_A^- can lower the energy of $P^+B_A^-$ with respect to that of P* thus stopping the coherent oscillations in the system and providing stabilization of $P^+B_A^-$. The exchange of TyrM210 by L or W blocks of the stabilization of the product $P^+B_A^-$.

To distinguish between these two possibilities (i) and (ii) a double mutation YM210L/HL168L was performed. The second mutation decreases the redox potential of the couple P/P^+ by −120 mV and therefore provides a lower energy position of $P^+B_A^-$ with respect to that of P*. Figs. 4 and 5 show for the P* (940 nm) and B_A^- (1020 nm) kinetics that in the double mutant a stabilization is still not observed in the ps time domain. Therefore the second possibility (ii) is the more realistic mechanism for the stabilization of the product $P^+B_A^-$ due to the motion of $H^{\delta+}$ of OH-TyrM210 toward B_A^- within the ps time domain.

4.1.2. (B) Photosystem II of green plants

In RCs of PSII the formation of the charge transfer state appears to occur upon excitation. The experimental data for that are described below.

Two lines of the experiments were used to study the mechanism of the primary charge separation in PSII. It was

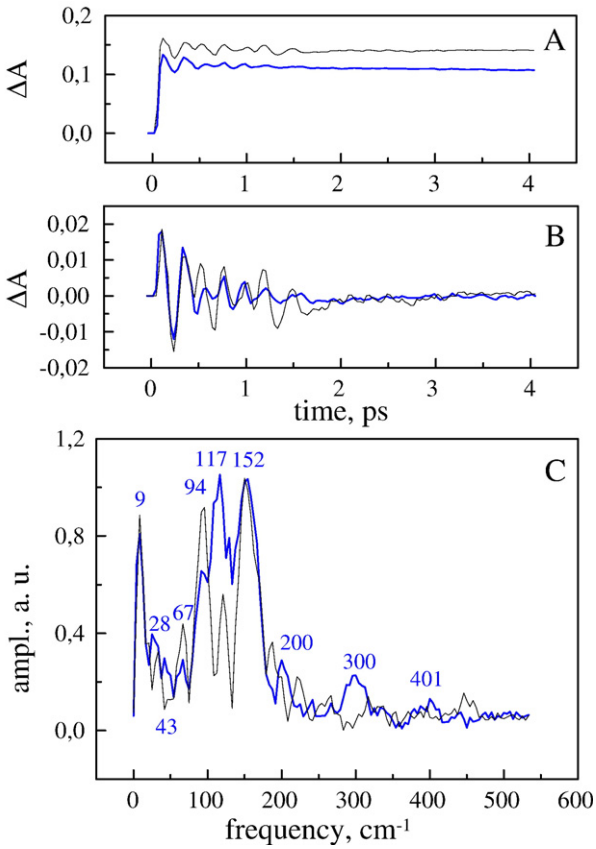

Fig. 4. Femtosecond kinetics of ΔA (A), its oscillatory part (B) and the spectrum of Fourier transform of the oscillatory part (C) for the 940-nm band in RCs of mutant YM210L (thin) and double mutant YM210L/HL168L (thick) of *Rb. sphaeroides* in glycerol-TT buffer at 90 K. RCs were excited by 18-fs pulses at 870 nm. (From Yakovlev et al., 2007, in preparation).

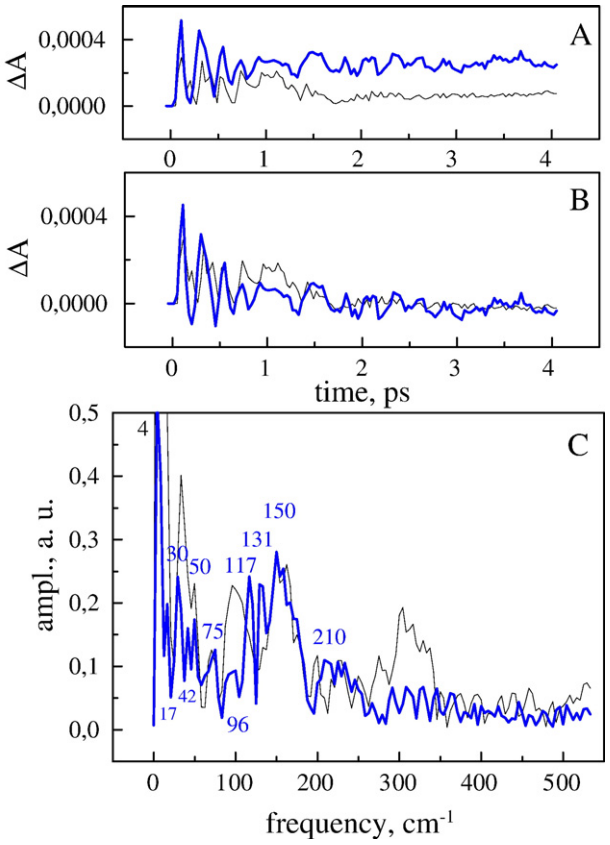

Fig. 5. Femtosecond kinetics of ΔA (A), its oscillatory part (B) and the spectrum of Fourier transform of the oscillatory part (C) for the 1020-nm band in RCs of mutant YM210L (thin) and double mutant YM210L/HL168L (thick) of *Rb. sphaeroides* in glycerol-TT buffer at 90 K. RCs were excited by 18-fs pulses at 870 nm. (From Yakovlev et al., 2007, in preparation).

shown by using electric field effects on Chl [27] that the Stark spectrum of the red-most absorbing Chl is considerably red-shifted as compared to the second derivative of the absorption spectrum. These data were explained in terms of a mixing of exciton states with a charge transfer state of about equal energy. It was suggested that the charge transfer state (CT) involves pheophytin molecule ($Pheo_{D1}$) and intermediate Chl_{D1}. The state $Chl^{+}_{D1}Pheo^{-}_{D1}$ was concluded to play a crucial role in the primary charge separation in PSII.

Similar conclusion was achieved using fluorescence measurements (Shuvalov, Heber, in preparation) on spinach leaves. It was found that two bands of variable fluorescence (ΔF) are observed in ΔF spectrum at 690 nm and 740 nm when Q_A is photoreduced. The temperature dependence for these two bands showed different slopes with 0.308 eV (690 nm) and 0.188 eV (740 nm), respectively, corresponding to ΔH changes when the state $P680^{+}Pheo^{-}_{D1}$ is activated by heat to P680*. These changes appear to be close to ΔG^{o} changes and can represent the energy position of $P680^{+}Pheo^{-}_{D1}$ with respect to two fluorescent centers having 0–0 transition at 685 nm (1.81 eV) and at 732 nm (1.69 eV). The fluorescence at 690 nm appears to demonstrate an excitation decay to the ground state. Taking into account that the red-shifted absorption of Chl has enhanced Stark effect [27] the fluorescence at 740 nm can be assigned to the transition from the charge transfer state, probably $Chl^{+}_{D1}Pheo^{-}_{D1}$, to the ground state (Fig. 6). In this case the transition occurs with dipole strength estimated to be ~5 times lower than that for Chl

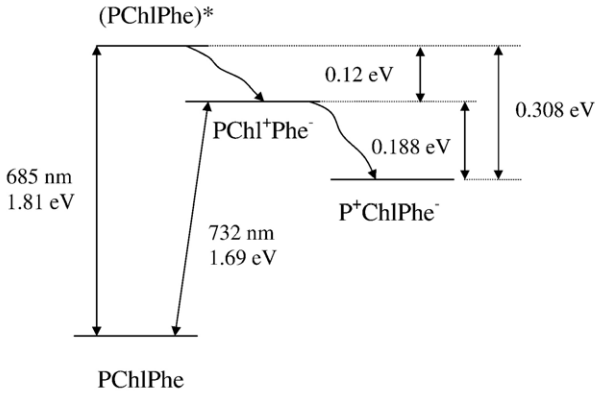

Fig. 6. Energy scheme of the primary events in PSII RCs. The excited state (PChlPhe)* (where P is P_{D1}–P_{D2}, Chl is Chl_{D1}, Phe is $Pheo_{D1}$) emitting at 690 nm is converted to the charge transfer state $PChl^{+}Phe^{-}$ which has a fluorescent transition to the ground state at 740 nm. The energy position of the charge separated state $P^{+}ChlPhe^{-}$ is lower than that of (PChlPhe)* by 0.308 eV and of $PChl^{+}Phe^{-}$ by 0.188 eV. (From Shuvalov and Heber, 2007, in preparation).

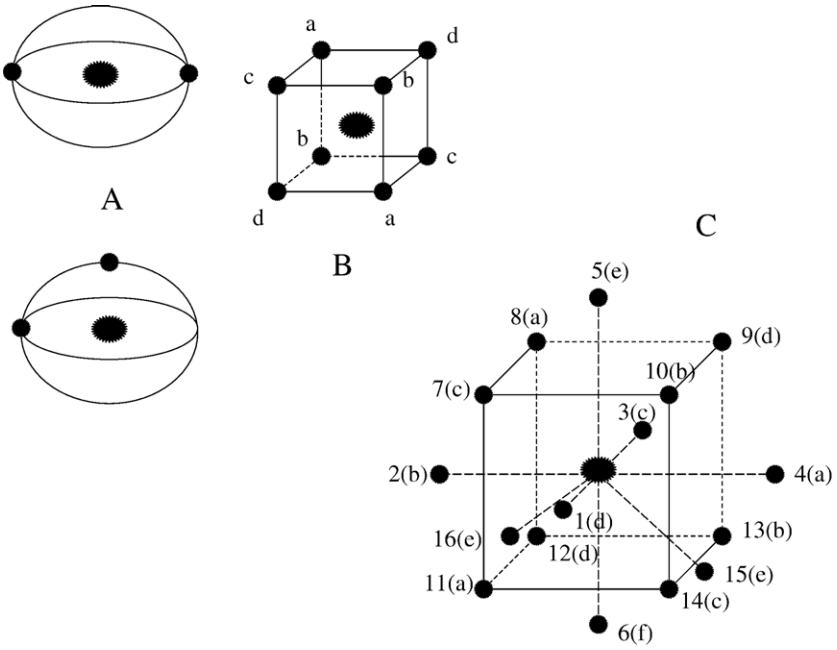

Fig. 7. The maximal localization of an electron density (small spheres) in many-electron atoms in 3D space for two orthogonal electron–photon orbits with $n=1$ (A), for four orbits (a, b, c, d) with $n=2$ (B), and for six orbits (a, b, c, d, e, f) with $n=3$ (C). In the center of the atom a thick sphere depicts the nucleus. (From Shuvalov [9,10]).

molecule. The contribution of the red-most absorption of spinach leaves to the reduction of terminal acceptor Q_A in RCII supports this idea [28].

Most interesting contribution to this field of the study was done by Hughes et al. [29]. The illumination of oxygen-evolving PSII core complexes at 1.7 K was found to lead to the reduction of Q_A. This reduction was induced not only in the central band at 685 nm but in the band at 700–730 nm which is far away from the chlorophyll absorption. The dipole strength of 0.15 Chl *a* was found near 705 nm. This finding was attributed to an indication of (i) strongly exciton-coupled RC excitation and of (ii) charge-transfer excitation in RC of the complex. The view of the balancing of electron and excitation energy transfer processes in PSII was described in [30].

The review of current state of knowledge on the primary electron transfer in PSII was presented in [31]. In agreement with previous discussion the evidences were presented that in the first electron transfer event the Chl_{D1} molecule transfers an electron from its excited singlet state to an $pheophytin_{D1}$ molecule which act as the primary electron acceptor with the formation of $Chl^{+}_{D1}Pheo^{-}_{D1}$. This event is followed by rapid spin redistribution, leading to predominant localization of the electron hole on P680 with the formation of the state $P680^{+}Pheo^{-}_{D1}$.

Thus, the mechanism of charge separation in RCs of PSII consists, probably, in the formation of the excited state in a core complex including antenna and RC Chl, followed by the formation of the charge transfer state $Chl^{+}_{D1}Pheo^{-}_{D1}$. Since the dipole strength for CT is only ~0.15 Chl, the main rout for the light energy conversion occurs via the Chl excited state relaxed to the CT state and accompanied by two fluorescence emissions at 690 nm from the excited state and at 740 nm from the CT state.

Acknowledgments

I would like to acknowledge very useful discussion with Prof. G. Renger, Prof. V.A. Skulachev, Prof. F.F. Litvin and Dr. N.D. Gudkov. This work was supported by FS and MCB grants from the Russian Academy of Sciences, grants from the Russian Foundation for Basic Research (05-04-48554à), grant from Ministry of education and science of RF, NWO grant 047-009-008 for Russian-Dutch Scientific Cooperation, INTAS grant 00-0404.

Appendix A

To use Eq. (8) it is necessary to find the value of the expression $\Sigma_i \Sigma_j r/r_{ij}$ where r is a distance between electrons with $n=n_e$ and the nucleus, r_{ij} is distances between electrons. To get the value of $\Sigma_i \Sigma_j r/r_{ij}$ one should find a maximal probability of the location of electrons in many-electron atom (the wave function in quantum mechanics).

As discussed in the text, an increase of n leads to an increase of the number of photon waves (proportional to $2n^2$) and an increase of λ for each orbit (proportional to n^2) with constant total photon energy emitted by the nucleus. For $n=1$ and $Z=1$ two electron–photon orbits, corresponding to the emission of two virtual photons with total energy of 2·3727 eV = 7454 eV, accept two electrons. For $n=2$ eight photon waves are able to accept eight electrons. For $n=3$ eighteen waves accept eighteen electrons, and so on.

On the other hand, since the photon spin is $\hbar$, one can suggest that this spin is exchanged with the orbit angular momentum (getting the same $\hbar$) of an electron ($n=1$) trapped by the photon electromagnetic field. For an electron with $n>1$ the

electron angular momentum is $n\hbar$. It means that for electrons with $n=2$ two photon spins are exchanged with the electron angular momentum, for $n=3$ three photon spins are exchanged with the electron angular momentum, and so forth. This feature is not simple since for $n=2$ we have claimed that 8 photon waves (energy of emitted photons is $8\cdot3727/n^2=7454$ eV) accept 8 electrons but at the same time two photon spins are exchanged with one electron angular momentum. It means that for $n=2$ two photon waves are interacting with the creation of one electron–photon orbit accepting two electrons with $L=2\ \hbar$. As a result there are 4 electron–photon orbits accepting 8 electrons with $n=2$. An analogous situation occurs for $n=3$ when 18 photon waves (energy of emitted photons is $18\cdot3727/n^2=7454$ eV) accept 18 electrons but three photon waves are interacting with the creation of one electron–photon orbit accepting three electrons with $L=3\ \hbar$. As a result there are six electron–photon orbits accepting 18 electrons with $n=3$, and so on. Please note that in all cases the total photon energy emitted by the nucleus is constant and equal to 7454 eV (see above).

The mutual arrangement of the electron–photon orbits was found to follow the standard tendency to be orthogonal as possible since only in this case the Coulomb repulsion energy for interacting electrons is minimal. Another tendency is related to the maximal probability to find an electron in the points of an interference of the electron–photons orbits. As a result for four electron–photon orbits ($n=2$) the crossing points are located in the corners of cub representing the location of 8 electrons (Fig. 7B). For six electron–photon orbits ($n=3$) the crossing points are located in the corners of the rectangular parallelogram representing the location of 8 electron of Ar and other 10 points (for Kr) are located as shown in Fig 7C [9,10], etc. A reasonable result is obtained by the suggestion [9,10] that two electrons with $n=1$ move synchronously on two orthogonal orbits to get minimal potential energy. For this case two predominant locations for two electrons with angle of 90° and of 180° with the nucleus in the center are in good correlation with experiment (Fig. 7A).

To get the value of $\Sigma_i\ \Sigma_j\ r/r_{ij}$ one should find the distances in the figures depicted in Fig. 7 for each couple of electrons, take a ratio of r/r_{ij} for these couples and calculate a sum.

References

[1] L.D. Landau, E.M. Lifshits, Quantum Mechanics, Non-Relativistic Theory (Theoretical Physics, v.3), Nauka, Moscow, 1974.

[2] R. Eisberg, R. Resnick, Quantum Physics of Atoms, Molecules, Solids, Nuclei, and Particles, Wiley, NY, 1985.

[3] P.A.M. Dirac, The Principles of Quantum Mechanics, Clarendon Press, Oxford, 1986.

[4] J.J. Sakurai, Modern Quantum Mechanics, Addison-Wesley, Reading, MA, 1994.

[5] Y. Ishikawa, H.M. Quiney, G.L. Malli, Dirac-Fock- Breit self-consistent-field method: Gaussian basis-set calculations on many-electron atoms, Phys. Rev., A 43 (1991) 3270–3278.

[6] R.P. Feynman, Space-time approach to quantum electrodynamics, Phys. Rev. 76 (1949) 769–789.

[7] R.P. Feynman, QED, The Strange Theory of Light and Matter, Princeton Univ. Press, Princeton, NJ, 1985.

[8] A.I. Akhieser, V.B. Berestetsky, Quantum Electrodynamics, Nauka, Moscow, 1981.

[9] V.A. Shuvalov, Quantum dynamics of electrons in many-electron atoms of biologically important compounds, Biochemistry (Mosc.) 68 (2003) 1333–1354.

[10] V.A. Shuvalov, Quantum dynamics of electrons in atoms of biologically important molecules, Uspekhi biologicheskoi khimii, (Pushchino) 44 (2004) 79–108.

[11] D.R. Lide (Ed.), CRC Handbook of Chemistry and Physics, CRC Press, Boston, 2003.

[12] Yu.A. Vladimirov, D.I. Roshchupkin, E.E. Fesenko, Photochemical reaction in amino-acid residues and inactivation of enzymes during UV-irradiation, Photochem. Photobiol. 11 (1970) 227–246.

[13] R.A. Marcus, N. Sutin, Electron transfer in chemistry and biology, Biochim. Biophys. Acta 811 (1985) 265–322.

[14] A.N. Terenin, Photonics of Dye Molecules, Nauka, Moscow, 1967.

[15] H. Beens, A. Weller, Excited molecular π-complexes in solution, in: J.B. Birks (Ed.), Organic Molecular Photophysics, vol. 11, John Wiley & Sons, London, 1975, pp. 159–215.

[16] H. Michel, O. Epp, J. Deisenhofer, Pigment–protein interactions in the photosynthetic reaction centre from *Rhodopseudomonas viridis*, EMBO J. 5 (1986) 2445–2451.

[17] H. Komiya, T.O. Yeates, D.C. Rees, J.P. Allen, G. Feher, Structure of the reaction center from *Rhodobacter sphaeroides* R-26 and 2.4.1: symmetry relations and sequence comparisons between different species, Proc. Natl. Acad. Sci. U. S. A. 85 (1988) 9012–9016.

[18] A.G. Yakovlev, A.Ya. Shkuropatov, V.A. Shuvalov, Nuclear wave packet motion between P* and $P^+B_A^-$ potential surfaces with subsequent electron transfer to H_A in bacterial reaction centers: 1. Room temperature, Biochemistry 41 (2002) 2667–2674.

[19] A.G. Yakovlev, A.Ya. Shkuropatov, V.A. Shuvalov, Nuclear wave packet motion between P^* and $P^+B_A^-$ potential surfaces with a subsequent electron transfer to H_A in bacterial reaction centers at 90 K. Electron transfer pathway, Biochemistry 41 (2002) 14019–14027.

[20] M.H. Vos, M.R. Jones, C.N. Hunter, J. Breton, J.-C. Lambry, J.-L. Martin, Coherent dynamics during the primary electron-transfer reaction in membrane-bound reaction centers of *Rhodobacter sphaeroides*, Biochemistry 33 (1994) 6750–6757.

[21] M.H. Vos, M.R. Jones, J. Breton, J.-C. Lambry, J.-L. Martin, Vibrational dephasing of long- and short-lived primary donor excited states in mutant reaction centers of *Rhodobacter sphaeroides*, Biochemistry 35 (1996) 2687–2692.

[22] A.G. Yakovlev, T.A. Shkuropatova, L.G. Vasilieva, A.Ya. Shkuropatov, P. Gast, V.A. Shuvalov, Vibrational coherence in bacterial reaction centers with genetically modified B-branch pigment composition, Biochim. Biophys. Acta 1757 (2006) 369–379.

[23] T.R. Middendorf, L.T. Mazzola, K.O. Lao, M.A. Steffen, S.G. Boxer, Stark effect (electroabsorption) spectroscopy of photosynthetic reaction centers at 1.5 K — evidence that the special pair has a large excited state polarizability, Biochim. Biophys. Acta 1143 (1993) 223–234.

[24] A.G. Yakovlev, L.G. Vasilieva, A.Ya. Shkuropatov, T.I. Bolgarina, V.A. Shkuropatova, V.A. Shuvalov, Mechanism of charge separation and stabilization of separated charges in reaction centers of *Chloroflexus aurantiacus* and of YM210W(L) mutants of *Rhodobacter sphaeroides* excited by 20 fs pulses at 90 K, J. Phys. Chem., A 107 (2003) 8330–8338.

[25] A. Kuglstatter, P. Hellwig, G. Fritzsch, J. Wachtveitl, D. Oesterhelt, W. Mantele, H. Michel, Identification of a hydrogen bond in the Phe M197→Tyr mutant reaction center of the photosynthetic purple bacterium *Rhodobacter sphaeroides* by X-ray crystallography and FTIR spectroscopy, FEBS Lett. 463 (1999) 169–174.

[26] C. Rischel, D. Spiedel, J.P. Ridge, M.R. Jones, J. Breton, J.-C. Lambry, J.-L. Martin, M.H. Vos, Low frequency vibrational modes in protein: charges induced by point-mutations in the protein-cofactor matrix of bacterial reaction centers, Proc. Natl. Acad. Sci. U. S. A. 95 (1998) 12306–12311.

[27] R.N. Frese, M. Germano, F.L. de Weerd, I.H.M. van Stokkum, A.Ya. Shkuropatov, V.A. Shuvalov, H.J. van Gorkom, R. van Grondelle, J.P. Dekker, Electric field effects on the chlorophyll, pheophytins, and β-carotenes in the reaction center of photosystem II, Biochemistry 42 (2003) 9205–9213.

[28] U. Heber, V.A. Shuvalov, Photochemical reactions of chlorophyll in

dehydrated photosystem II: two chlorophyll forms (680 and 700 nm), Photosynth. Res. 84 (2005) 84–91.
[29] J.L. Hughes, P. Smith, R. Pace, E. Krausz, Charge separation in photosystem II core complexes induced by 690–730 excitation at 1.7 K, Biochim. Biophys. Acta 1757 (2006) 841–851.
[30] L.M.C. Barter, J.R. Durrant, D.R. Klug, A quantitative structure–function relationship for the Photosystem II reaction centers: supermolecular behavior in natural photosynthesis, Proc. Natl. Acad. Sci. U. S. A. 100 (2003) 946–951.
[31] G. Renger, A.R. Holzwarth, Primary electron transfer, in: T. Wydrzynski and K. Satoh (Eds.), Photosynthesis II: The Light-Driven Water:Plastoquinone Oxidoreductase, Springer, The Netherlands, 2006, pp. 139–175.
[32] Atomic radius, The university of Sheffield and Webelements LTD, UK (2006) (www.webelements.com).